Iğdır Üniversitesi Fen Bilimleri Enstitüsü Dergisi, 11(3): 2184-2194, 2021
Journal of the Institute of Science and Technology, 11(3): 2184-2194, 2021

ISSN: 2146-0574, eISSN: 2536-4618

Kimya / *Chemistry* **DOI: 10.21597/jist.941474**

Araştırma Makalesi / *Research Article*

Geliş tarihi / Received: 23-05-2021 **Kabul tarihi / Accepted: 05-06-2021**

To Cite: Altınölçek N, Battal A, 2021. The Investigation of Fluorescence Biothiol Sensor Properties of 2-(N-hexyl-carbazole-3'-yl)-4-formylpyridine. Journal of the Institute of Science and Technology, 11(3): 2184-2194.

The Investigation of Fluorescence Biothiol Sensor Properties of 2-(N-hexyl-carbazole-3'-yl)-4-formylpyridine

Nuray ALTINOLCEK[1*], Ahmet BATTAL[2]

ABSTRACT: The biothiol sensor properties of 2-(N-hexyl-carbazole-3'-yl)-4-formylpyridine molecule were examined. This probe has carbazole moiety as a fluorophore and aldehyde group as a recognition site. Three different biothiol molecules as an analytes were chosen that they are cysteine (Cys), homocysteine (Hcy) and glutathione (GSH). We monitored the adduct formation between probe and analyte (biothiols) by ^{1}H NMR, MS, UV-vis and PL Spectrometers.

Keywords: Aldehyde group, Carbazole, Cysteine, Glutathione, Homocysteine, Biothiol sensor

[1] Nuray Altinolcek (**Orcid ID:** 0000-0002-9553-1474), Uludag University, Faculty of Science-Art, Department of Chemistry, 16059 Nilufer, Bursa, Turkey
[2] Ahmet Battal (**Orcid ID:** 0000-0003-0208-1564), Mus Alparslan University, Faculty of Education, 49100, Mus, Turkey

***Sorumlu Yazar/Corresponding Author:** Nuray ALTINÖLÇEK, e-mail: nurayaltinolcek@hotmail.com

Bu çalışmada adı geçen "probe 1", oled çalışmaları kapsamında siklometalleme ligandı (8a) olarak Nuray ALTINÖLÇEK'in doktora tez kapsamında sentezlenmiş olup, 8a'nın sentezi Beilstein Journal of Organic Chemistry (2020, 16, 1066-1074) dergisinde 7a olarak yayınlanmıştır. Bu çalışmada ise 8a doktora tez çalışmasından farklı olarak "floresans biyotiyol sensörü" olarak ele alınmış ve bu özelliği UV, PL, NMR ve MS spektrumlarıyla incelenmiştir.

INTRODUCTION

Cysteine (Cys), homocysteine (Hcy) and glutathione (GSH) are important biothiol molecules for humans and they all play key roles in a number of physiological and pathological processes (Mahapatra et al., 2013; Peng et al., 2014; Wang et al., 2015; Wang et al., 2017; Song et al., 2018). Therefore, biothiol levels in human cells should be closely monitored in a practical way to avoid the worst consequences (Liu et al., 2015; Zhang et al., 2016; Wang et al., 2018). For these purposes, fluorescence spectroscopy is considered much practical due to its ease of use and sensitivity (Fu et al., 2017; Tong et al., 2017; Chai et al., 2018; Li et al., 2019). In this respect, a number of fluorescence probes have been designed and synthesised so far (Sok et al., 2017; Wang et al., 2021). A probe usually consists of a fluorophore and a recognition site (Mei et al., 2013; Zhang et al., 2020). Carbazole, coumarin etc. are frequently used as a fluorophore and chemical recognitions *via* a nucleophilic addition, Michael addition, nucleophilic aromatic substitution etc. is more preferred as a recognition site (Niu et al., 2012; Chen et al., 2017; Ding et al., 2018). Probe when mixed with a biothiol, upon excitation, should give one of the following changes in emissions; an increase in emission (turn-on) or a decrease in emission (turn-off) or a change in emission colors (blue-shift or red-shift) (Mei et al., 2013; Jang et al., 2015; Babür et al., 2016). These changes occur *via* a different emission mechanism. In this paper, we choose carbazole as a fluorophore and aldehyde group as a recognition site and from this we previously synthesised a probe: 2-(N-hexyl-carbazole-3'-yl)-4-formylpyridine **1** and reported literature by us (Altinolcek et al., 2020). We examined the adduct formation between probe **1** and biothiols by ^{1}H NMR, MS, UV-vis and PL spectrometers.

MATERIALS AND METHODS

Probe **1** was synthesised in four steps from carbazole as described previously (Altinolcek et al., 2020). Biothiols of Cys (L-Cysteine), Hcy (DL-Homocysteine) and GSH (L-Glutathione reduced) was ordered from Sigma Aldrich and were stored at the recommended temperature (Hcy: -20°C, Cys and GSH: +2-8°C). Nuclear magnetic resonance (NMR) spectra (^{1}H) were recorded on a Bruker Avance III (400 MHz) NMR spectrometer. NMR experiments were performed to explore the coordination sites and sensing mechanism between probe **1** and biothiols. Adduct formations were also confirmed by mass analysis using Bruker microTOFq mass spectrometers to obtain low- and high-resolution spectra using electrospray ionisation (ESI) with positive ion mode. UV and PL were measured on a Duetta two-in-one fluorescence and absorbance spectrometer from Horiba Scientific. Solutions used in this study were prepared as follows.

Probe 1 stock solution: Probe **1** (5.35 mg) was dissolved in DMSO (5.0 ml) to make a $3x10^{-3}$ M main stock solution. Due to insolubility of probe **1**, HEPES buffer solution was diluted with a DMSO in the ratio of 9:1 v/v.

HEPES buffer stock solution (1.0 L, 0.10 M, pH=7.4): A HEPES salt (23.8 g) was added to deionised water (900 ml) in volumetric flask and shaken until completely dissolved (~3 min). The initial pH of the solution, which was ~5, was carefully adjusted to 7.4 by dropwise addition of aqueous (deionised) NaOH solution (20% w/w, 25 ml). The pH was monitored by a pH meter. When the pH of the HEPES buffer solution was 7.4, volumetric flask was filled with deionised water till the volume was 1.0 L. The buffer was covered with aluminum foil and was stored in the refrigerator for the long-term use.

Analyte stock solution: Like probe **1**, to make $3x10^{-3}$ M analyte main stock solutions, Cys (3 mg/8.25 ml), Hcy (3 mg/7.4 ml) and GSH (8 mg/8.68 ml) were dissolved in HEPES buffer solution (0.1 M, pH=7.4).

Titration studies: The stock solution of $3x10^{-3}$ M for probe **1** was used. Analytes equivalences was varied from 0, 1, 5, 10, 20, 40, 60, 80 and 100, corresponding to 0 µl, 10 µl, 50 µl, 100 µl, 200 µl, 400 µl, 600 µl, 800 µl and 1000 µl, respectively. For each titration, a 10 µl of probe **1** and a required amount of analytes were mixed together and then the mixture were diluted to a final volume of 3.0 ml. This gave the final concentration of probe **1** as $1.0x10^{-5}$ M. The final analytes concentration changed from 0 to $1x10^{-3}$ M. OD and PL of each resulting solutions (maximum at 516 nm) were measured after shaking for 20 mins.

NMR solutions: 9.35 mM stock solution of probe **1** and biothiols were prepared in deuterated dimethyl sulfoxide (DMSO-d_6) and in deuterated water (D_2O), respectively. A solution of probe **1** was prepared in deuterated dimethyl sulfoxide (DMSO-d_6, 0.6 ml) by dissolving ca. 2 mg of 1. This solution was taken in the NMR tube. A biothiol solution, prepared in deuterated water (D_2O, 0.6 ml) by dissolving a suitable equivalent, was added to the NMR tube.

RESULTS AND DISCUSSION

Photophysical properties

First of all, absorption and emission properties of probe **1** in DMSO:HEPES buffer solution (1:9 v/v, pH=7.4) were investigated by UV-Vis and fluorescence spectroscopy, respectively (Figure 1). Probe **1** displayed similar absorption and emission profiles as reported previously (Altinolcek et al., 2020) in DCM and different solvents. In UV-vis, high-energy bands and mid-energy bands were assigned to π-π* and n-π* transitions, whereas low-energy bands were assigned to intramolecular charge transfer (ICT) transition. Upon excitation at ICT band (λ_{exc}=374 nm), probe **1** displayed a single emission band at 516 nm due to ICT state. In sensor studies, we choose ICT absorption intensity change at 374 nm and emission intensity change at 516 nm.

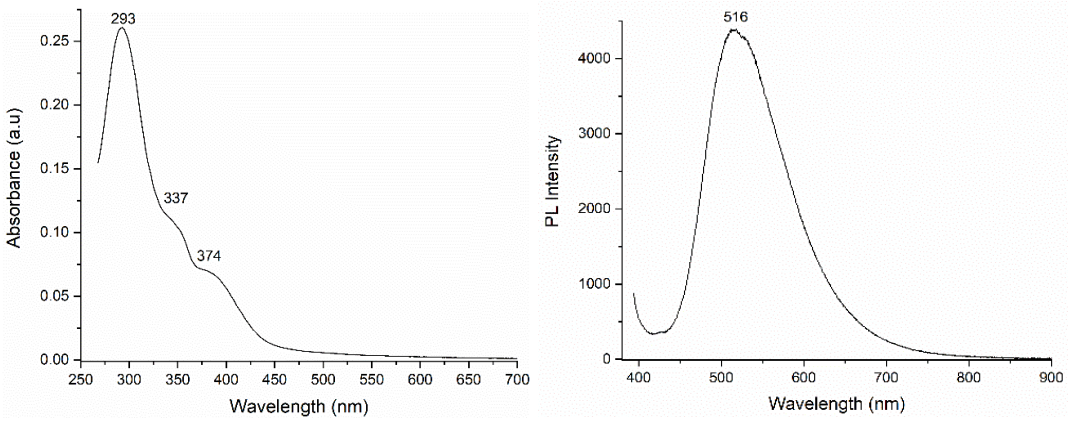

Figure 1. UV-vis and PL spectra of probe **1** in DMSO:HEPES buffer solution (1:9 v/v, pH=7.4)

Sensor properties

To investigate sensor properties of probe **1**, initially, three different analytes were chosen; cysteine (L-Cys), homocysteine (DL-Hcy) and glutathione (L-GSH). To begin sensor studies, two things should be determined at the onset; solvent systems and probe concentration range. A mixture of dimethyl sulphoxide (DMSO) and HEPES buffer (0.1 M, pH=7.4) was chosen as solvent systems, in where both probe and analytes were soluble. In addition to that, this solvent system is frequently used in pharmacological and biological studies (Mahapatra et al., 2013; Zhai et al., 2013; Kaur et al., 2014;

Hu et al., 2015). To determine the best solvent system solvent fraction ratio was optimised. For this probe **1** were dissolved in a different fractions (from 1:9 to 9:1) of DMSO:HEPES buffer solutions and then their absorption and emission behaviours were investigated. From this, a 1:9 fraction ratio of DMSO:HEPES buffer solution was determined as the best solvent system since the emission intensity was highest and emission profile was cleanest at 516 nm (Figure 2a). Once solvent fraction was determined attention was turned to determination of probe concentration range, in where no aggregation occurs and PL change with concentration obeys Beer-Lambert law. For this, 25 different concentrations of probe **1** were prepared in DMSO/HEPES buffer (1:9 v/v, pH=7.4) solution. For each concentration, probe **1** solution was excited at 374 nm and emission spectrum was recorded as shown in Figure 2b. As concentration of probe **1** increased from 0 to $20x10^{-5}$ M emission intensity at 516 nm increased linearly (Figure 2c) and further increase in concentration of probe **1** from $20x10^{-5}$ M to $70x10^{-5}$ M resulted in a decrease in emission intensity at 516 nm due to aggregation. Hence for titration studies a concentration value of $1.0x10^{-5}$ M for probe **1** was chosen.

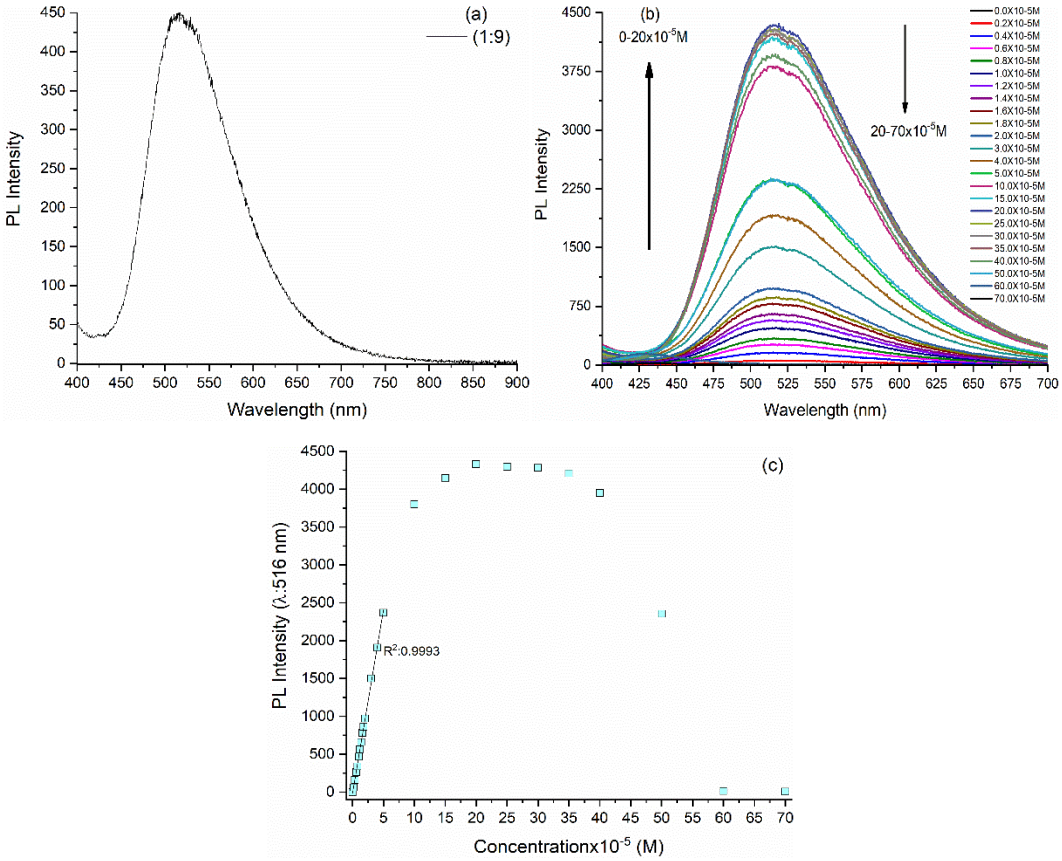

Figure 2. (a) PL graph of probe **1** in a mixture of 1:9 DMSO:HEPES buffer solution, **(b)** PL graph of probe **1** at different concentrations and **(c)** PL intensity at 516 nm-concentration of probe **1** graph in a mixture of 1:9 DMSO:HEPES buffer solution

Photostability and reaction time

First of all photostability of probe **1** was determined. For this, changes in optical density at 374 nm (OD_{374}) and emission intensity (I_{516}) at emission maxima of probe **1** was recorded over a time period of 1800 seconds in a 1:9 mixture of DMSO and HEPES buffer (0.1 M, pH=7.4) solution without any analytes. Secondly, reaction time was determined by adding 10 and 60 equivalents of analytes and then recording changes at OD_{374} and I_{516} over a time period of 1800 seconds. The OD_{374} /I_{516}-time graphs were depicted in Figure 3.

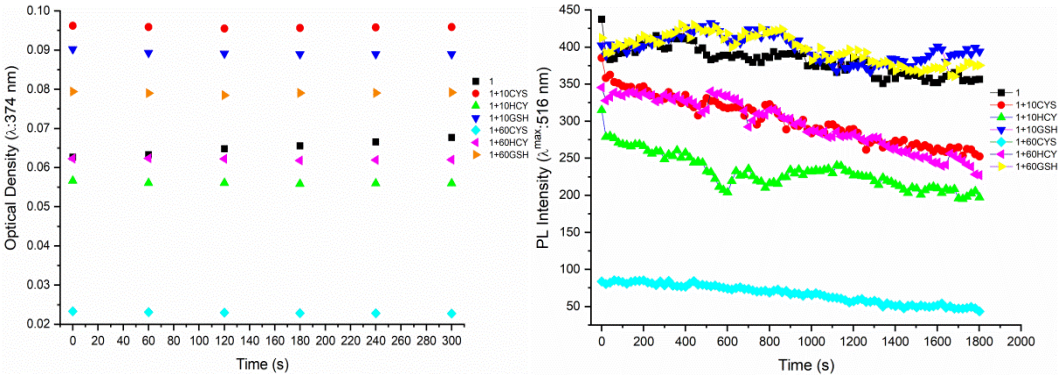

Figure 3. OD_{374}-time and I_{516}-time graphs of probe **1**

OD_{374} of free probe **1** shows a tendency to increase slightly from 0.063 to 0.067 over a time period of 300 seconds. In contrast to absorption, emission intensity (I_{516}) of free probe **1** at 516 nm shows a tendency to decrease slightly from 375 to 350 over a time period of 1800 seconds. Hence **1** can be considered a stable probe.

Upon addition of 10 equivalents of Cys, OD_{374} of the mixture (**1**+10 Cys) increased to 0.095, but upon addition of 60 equivalents of Cys, OD_{374} of the mixture (**1**+60 Cys) sharply decreased to 0.024. In both cases, OD_{374} remained constant over a time period of 5 min. This indicates that probe **1** had reacted with Cys by following different reaction kinetics. Upon addition of 10 equivalents of Hcy, OD_{374} of the mixture (**1**+10 Hcy) slightly decreased to 0.056, but upon addition of 60 equivalents of Hcy, OD_{374} of the mixture (**1**+60 Hcy) slightly increased back to 0.063, an identical OD_{374} of free probe **1**. In both cases, OD_{374} remained constant over time period of 5 min. This indicates that probe **1** just reacted very slightly with Hcy. Upon addition of 10 and 60 equivalents of GSH, OD_{374} of mixtures (**1**+10 GSH and **1**+60 GSH) increased to 0.090 and 0.080, respectively, and in both cases, OD_{374} remained constant over time period of 5 min. This indicates that probe **1** reacted slightly with GSH.

Upon addition of 10 equivalents of Cys, I_{516} of the mixture (**1**+10 Cys) slightly reduced to 350, but upon addition of 60 equivalents of Cys, I_{516} of the mixture (**1**+60 Cys) sharply reduced to 80. In both cases, reduction continued over a time period of 30 min. This indicates that probe **1** had reacted with Cys by following different reaction kinetics. Upon addition of 10 equivalents of Hcy, I_{516} of the mixture (**1**+10 Hcy) decreased to 275, but upon addition of 60 equivalents of Hcy, I_{516} of the mixture (**1**+60 Hcy) slightly increased back to 325. In both cases, a similar trend was over a time period of 30 min. This indicates that probe **1** reacted slightly with Hcy. Upon addition of 10 and 60 equivalents of GSH, I_{516} of mixtures (**1**+10 GSH and **1**+60 GSH) remained constant at 375 and a similar trend was observed over a time period of 30 min. This indicates that probe **1** did not react with GSH.

Fluorescence titration studies

To further find out whether the changes in absorption and emission intensities were due to biothiols or water or buffer solution, UV and PL were also recorded by adding just water or just DMSO or by changing buffer solution. From these graphs, it was clear that there were fluctuations in absorption and emission (Figure 4).

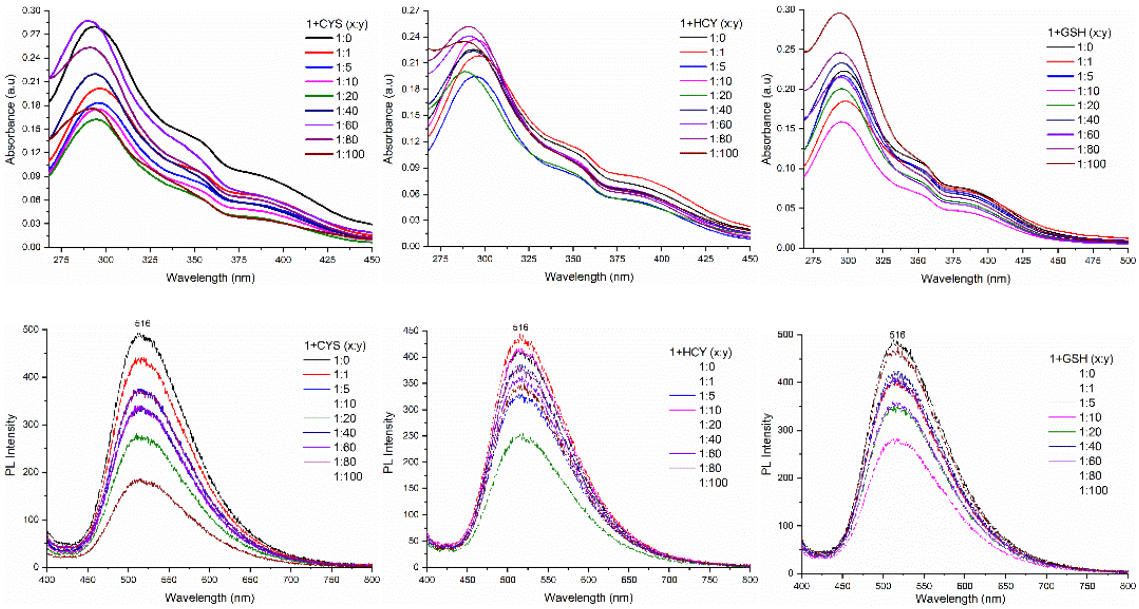

Figure 4. UV and PL graphs of **1-Cys, 1-Hcy** and **1-GSH** adducts in a 1:9 mixture of DMSO-HEPES buffer solution (0.1 M, pH:7.4) at different equivalents

Reaction mechanism

It is well known that the reaction of aldehydes with L-cysteine (Cys), DL-homocysteine (Hcy) and glutathione (GSH) forms cyclic N,S-acetals. In general Cys generates five-membered 1,3-thiazolidine ring (Baert et al., 2015), Hcy generates six-membered 1,3-thiazinane ring (Yue et al., 2011; Kamps et al., 2019) and GSH generates ten-membered 7-oxo-1,3,8-thiadiazecane ring (Hopkinson et al., 2010). The ring formation can proceed *via* either imine formation or hemithioacetal formation. Recent work with formaldehyde suggests that the ring formation proceeds via hemithioacetal formation (Kamps et al., 2019).

In our case, we also monitored the adduct formation between probe **1** and biothiols by ^{1}H NMR and MS. Probe **1** reacted with Cys very fast and the reaction was complete with an addition of 3 equivalents of Cys. Whereas probe **1** reacted with Hcy slowly and was only complete with an addition of 10 equivalents of Hcy. However, probe **1** was only reacted with GSH by adding 16 equivalents of GSH. The reaction was still incomplete. All reactions were carried out in a mixture of deuterated dimethyl sulphoxide (DMSO-*d*6) and deuterated water (D_2O). Adducts (**1-Cys** and **1-Hcy**) were obtained as diastereoisomeric mixtures. **1-Cys** adduct was 2-substituted 1,3-thiazolidine-4-carboxylic acid and **1-Cys** adduct was 2-substituted 1,3-thiazanine-4-carboxylic acid. These reactions were depicted in Scheme 1.

For **1-Cys** adduct, stacked ^{1}H NMR spectra (Figure 5) indicate that the characteristic aldehyde peak of **1** at 10.2 ppm disappeared and new peaks belonging to 1,3-thiazolidine ring of **1-Cys** adduct appeared. A set of peaks were observed for each diastereoisomer; singlet at 5.79 ppm and 5.60 ppm (2-H), triplet at 4.24 ppm and 3.46 ppm (4-H) and multiplet between 3.31-3.42 ppm and 3.07-3.17 ppm (5-H). Unreacted excess Cys in a mixture of D_2O and DMSO- d6 gave doublet of doublet at 3.37 ppm, multiplet between 2.47-2.55 ppm and multiplet between 1.81-2.03 ppm. Deuterium exchange with the hydrogen of thiol, amine and carboxyl simplified ^{1}H NMR spectra. ESI-MS analysis of adduct **1-Cys** indicates a protonated molecular ion peak at m/z=460.20, which belongs to $[M+H]^+$ (Figure 6a). HRMS further confirms that adduct **1-Cys** has a structure of $C_{27}H_{30}N_3O_2S$, for which m/z (found)=460.2046 and m/z (calculated)=460.2053 with an error of 1.5 ppm (Figure 6b).

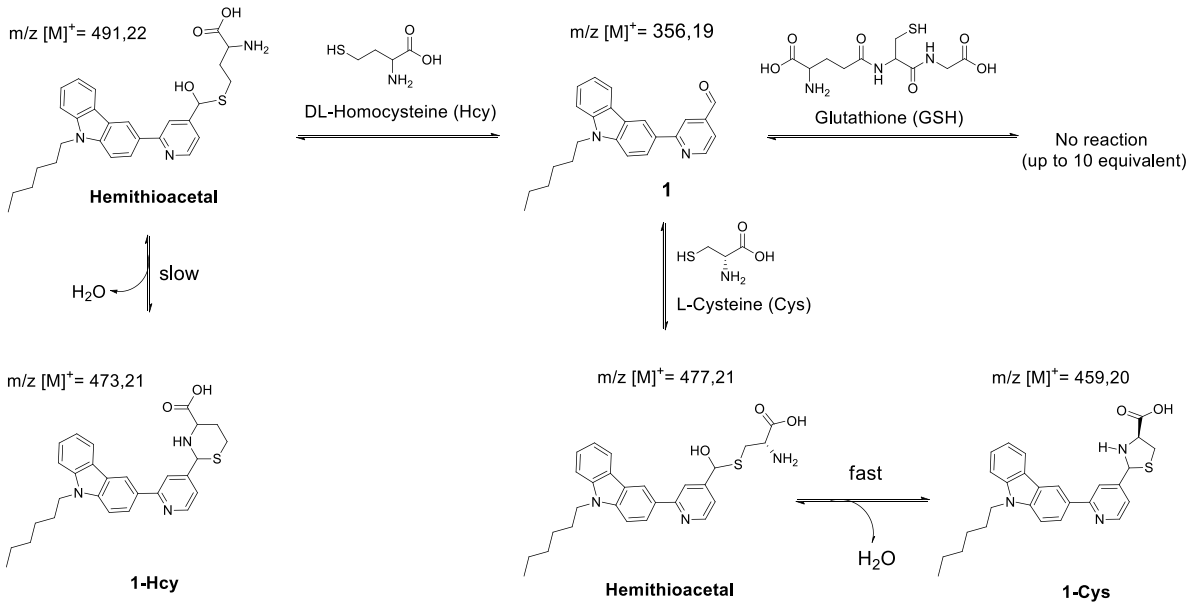

Scheme 1. Adduct formation between probe **1** and L-cysteine (Cys), DL-homocysteine (Hcy) and glutathione (GSH) *via* hemithioacetal

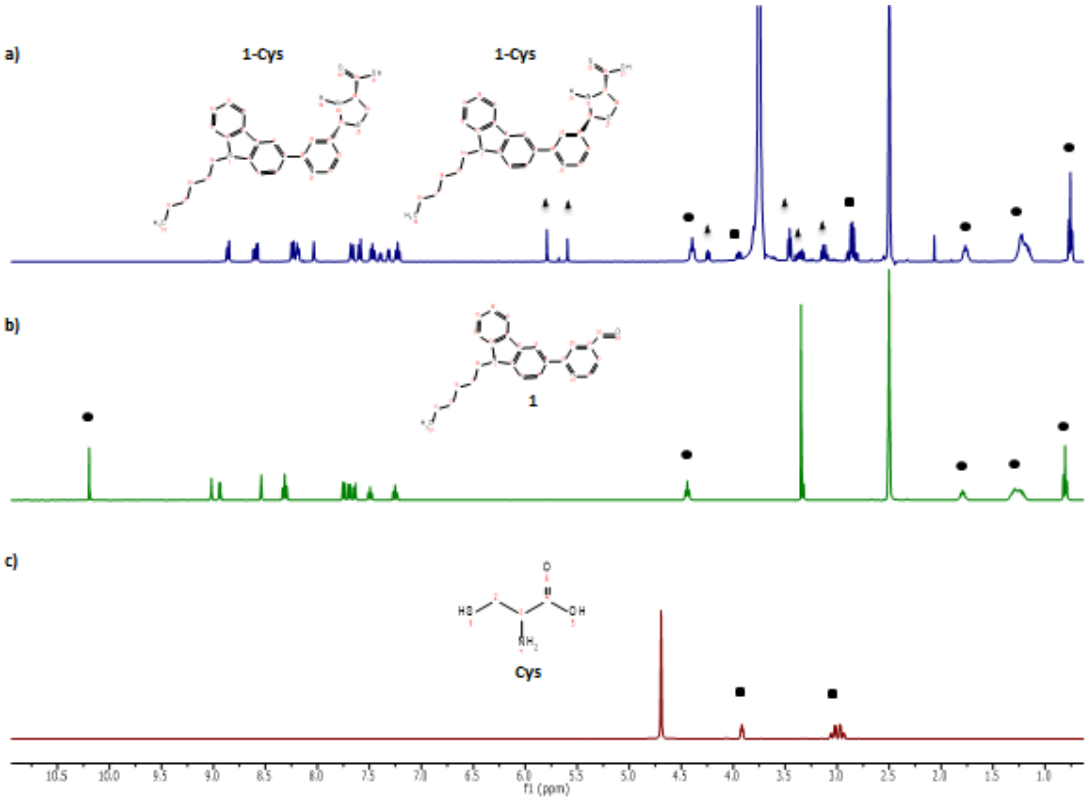

Figure 5. Stacked ^{1}H NMR spectra of **1-Cys** adduct **(a)**, probe **1 (b)** and cysteine-**Cys (c)**. Peaks assigned to **1-Cys** adduct is represented by solid triangle (▲), peaks assigned to probe **1** is represented by solid circle (●) and peaks assigned to cysteine (**Cys**) is represented by solid square (■)

For **1-Hcy** adduct, stacked ^{1}H NMR spectra (Figure 7) indicate that the characteristic aldehyde peak of **1** at 10.2 ppm disappeared and new peaks belonging to 1,3-thiazanine ring of **1-Hcy** adduct appeared. Predominantly a set of peaks were observed for only one diastereoisomer; singlet at 5.42 ppm (2-H), doublet at 3.55 ppm (4-H), triplet at 3.23 ppm (6-H), doublet at 2.92 ppm (6-H), doublet at 2.32 ppm (5-H), doublet at 1.15 ppm (5-H). Unreacted excess Hcy in D_2O gave triplet at 3.91 ppm, multiplet between 2.60-2.79 ppm and multiplet between 2.10-2.29. Deuterium exchange with the hydrogen of thiol, amine and carboxyl simplified ^{1}H NMR spectra. ESI-MS analysis of adduct **1-Hcy**

indicates a protonated molecular ion peak at m/z= 474.22, which belongs to $[M+H]^+$. HRMS further confirms that adduct **1-Hcy** has a structure of $C_{28}H_{32}N_3O_2S$, for which m/z (found)=474.2213 and m/z (calculated)=474.2210 with an error of -0.7 ppm (Figure 8).

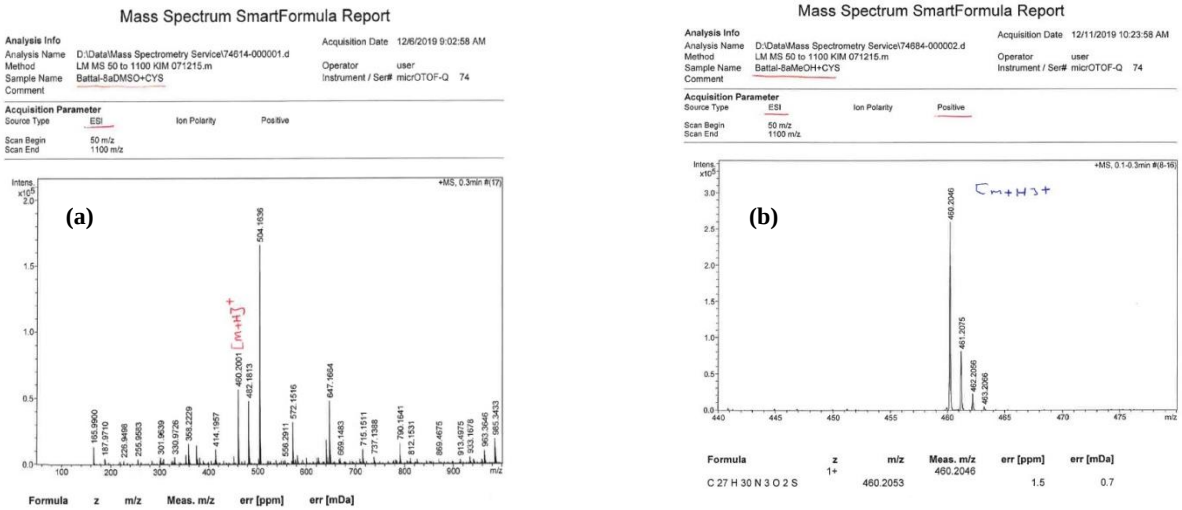

Figure 6. (a) MS spectrum of probe **1**-Cys adduct, **(b)** HRMS spectrum of probe **1**-Cys adduct

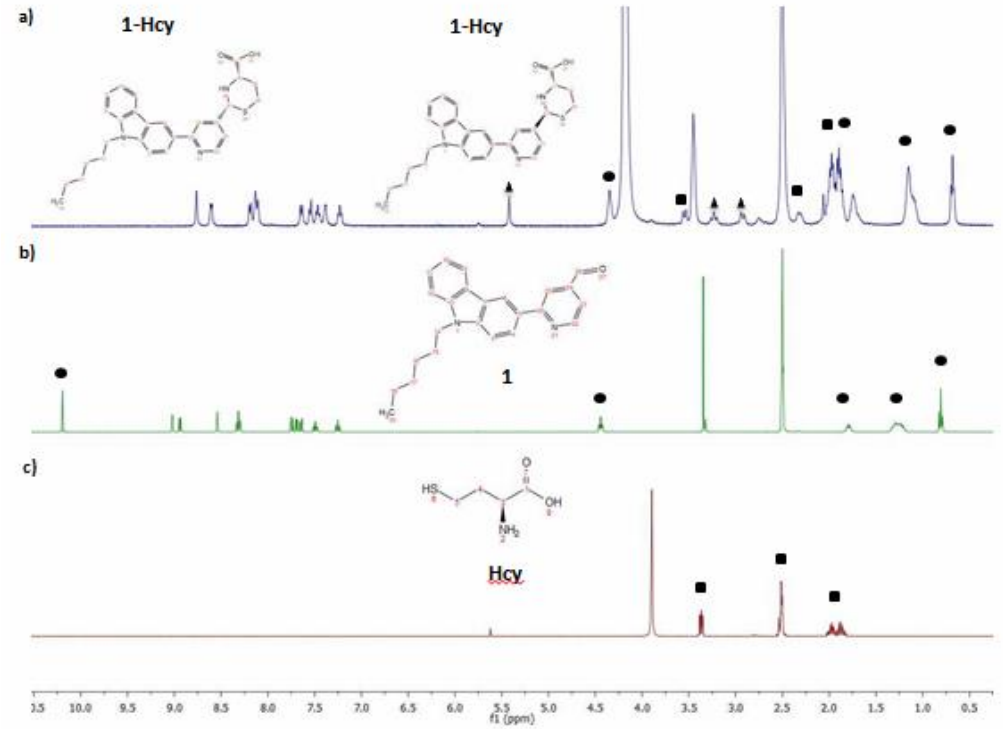

Figure 7. Stacked ^{1}H NMR spectra of **1-Hcy** adduct **(a)**, probe **1 (b)** and homocysteine-**Hcy (c)**. Peaks assigned to **1-Hcy** adduct is represented by solid triangle (▲), peaks assigned to probe **1** is represented by solid circle (●) and peaks assigned to homocysteine (**Hcy**) is represented by solid square (■)

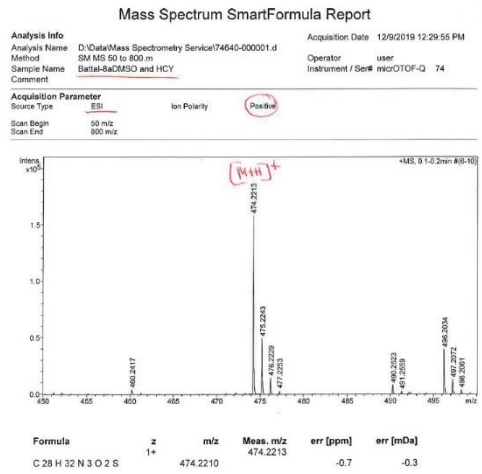

Figure 8. MS and HRMS spectrum of probe **1**-Hcy adduct

Probe **1** only reacted when 16 equivalents of GSH was used and ^{1}H NMR indicated that a tiny bits of characteristic aldehyde peak of **1** were present (Figure 9a). ESI-MS analysis of adduct **1-GSH** indicated adduct formation (Figure 9b).

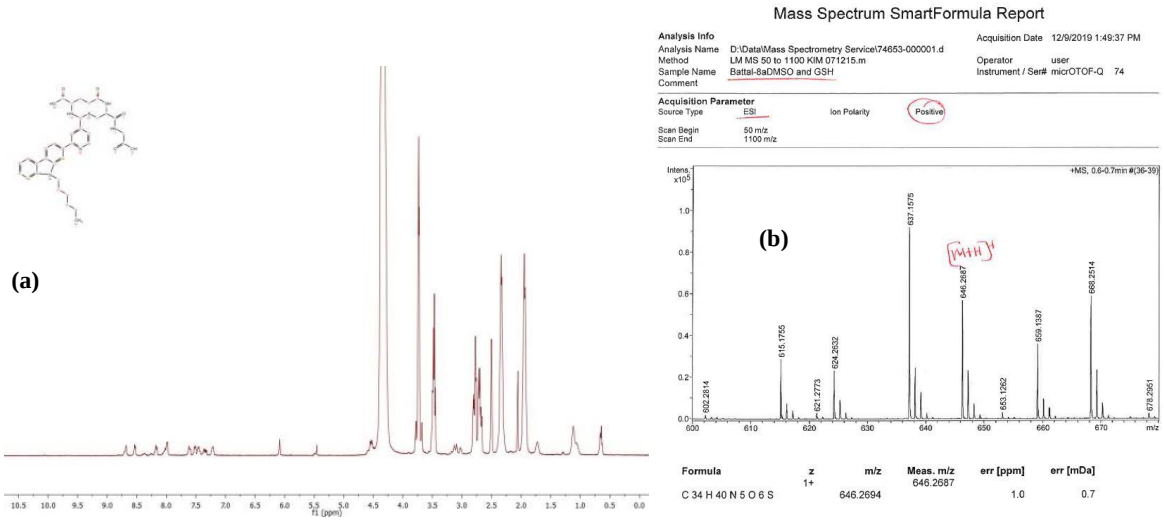

Figure 9. (a) ^{1}H NMR spectra of **1-GSH** adduct and **(b)** MS and HRMS spectrum of probe **1**-GSH adduct

CONCLUSION

In this work, we examined fluorescence sensor properties of probe **1** against biothiols. According to PL results, it could not be convincingly explained whether the changes in emission intensity were due to water or buffer solution or biothiols. These findings were also monitored by ^{1}H NMR and MS results. Further studies are needed to firmly establish the fluorescence sensing behaviour of probe **1**. However, these findings will still shed light on the design of new types of fluorescence biothiol sensors.

ACKNOWLEDGEMENTS

N. Altinolcek and A. Battal appreciate Prof. Dr. Mustafa Tavasli's valuable help and comments. A. Battal wants to thank TUBITAK-2219 Fellowship Programme (Grant Number:1059B191800354). A. Battal appreciates Prof. Dr. Peter J. Skabara's help for allowing to use his laboratory facilities and Dr. William Peveler's help for allowing to use Duetta Spectrometer. A. Battal also appreciates Dr. Oleksandr's helpful comments and Dr. Holly A. Yu's help for taking UV/PL spectra and Mr. Hao Yang's help for taking NMR Spectra.

Conflict of Interest

The authors declare that they have contributed equally to the article.

Author's Contributions

The article authors declare that there is no conflict of interest between them.

REFERENCES

Altinolcek N, Battal A, Tavasli M, Peveler WJ, Yu HA, Skabara PJ, 2020. Synthesis of novel multifunctional carbazole-based molecules and their thermal, electrochemical and optical properties. Beilstein Journal of Organic Chemistry, 16, 1066-1074.

Babür B, Seferoğlu N, Öcal M, Sonugur G, Akbulut H, Seferoğlu Z, 2016. A novel fluorescence turn-on coumarin-pyrazolone based monomethine probe for biothiol detection. Tetrahedron, 72(30), 4498-4502.

Baert JJ, De Clippeleer J, De Cooman L, Aerts G, 2015. Exploring the Binding Behavior of Beer Staling Aldehydes in Model Systems. Journal of the American Society of Brewing Chemists, 73(1), 100-108.

Chai G, Liu Q, Fei Q, Zhang J, Sun X, Shan H, Feng G, Huan Y, 2018. A selective and sensitive fluorescent sensor for cysteine detection based on bi-8-carboxamidoquinoline derivative and Cu2+ complex. Luminescence, 33(1), 153-160.

Chen C, Zhou L, Huang X, Liu W, 2017. Rapid detection of intracellular Cys over Hcy and GSH using a novel two-photon coumarinocoumarin-based colorimetric and fluorescent probe. Journal of Materials Chemistry B, 5(29), 5892-5897.

Ding S, Liu M, Hong Y, 2018. Biothiol-specific fluorescent probes with aggregation-induced emission characteristics. Science China Chemistry, 61(8), 882-891.

Fu Z-H, Han X, Shao Y, Fang J, Zhang Z-H, Wang Y-W, Peng Y, 2017. Fluorescein-Based Chromogenic and Ratiometric Fluorescence Probe for Highly Selective Detection of Cysteine and Its Application in Bioimaging. Analytical Chemistry, 89(3), 1937-1944.

Hopkinson RJ, Barlow PS, Schofield CJ, Claridge TDW, 2010. Studies on the reaction of glutathione and formaldehyde using NMR. Organic & Biomolecular Chemistry, 8(21), 4915-4920.

Hu Y, Heo CH, Kim G, Jun EJ, Yin J, Kim HM, Yoon J, 2015. One-Photon and Two-Photon Sensing of Biothiols Using a Bis-Pyrene-Cu(II) Ensemble and Its Application To Image GSH in the Cells and Tissues. Analytical Chemistry, 87(6), 3308-3313.

Jang G, Kim J, Kim D, Lee TS, 2015. Synthesis of triphenylamine-containing conjugated polyelectrolyte and fabrication of fluorescence color-changeable, paper-based sensor strips for biothiol detection. Polymer Chemistry, 6(5), 714-720.

Kamps JJAG, Hopkinson RJ, Schofield CJ, Claridge TDW, 2019. How formaldehyde reacts with amino acids. Communications Chemistry, 2(1), 126.

Kaur M, Yoon B, Kumar R, Cho Min J, Kim HJ, Kim JS, Choi DH, 2014. A Carbazole Based Bimodal "Turn-On" Fluorescent Probe for Biothiols (Cysteine/Homocysteine) and Fluoride: Sensing, Imaging and its Applications. Bulletin of the Korean Chemical Society, 35(12), 3437-3442.

Li C, Shang X, Chen Y, Chen H, Wang T, 2019. Biothiol detection by "ON-OFF-ON" fluorescence probe based on anthracene derivative. Journal of Molecular Structure, 1179, 623-629.

Liu T, Huo F, Yin C, Li J, Niu L, 2015. A highly selective fluorescence sensor for cysteine/homocysteine and its application in bioimaging. RSC Advances, 5(36), 28713-28716.

Mahapatra AK, Roy J, Sahoo P, Mukhopadhyay SK, Banik A, Mandal D, 2013. Carbazole phenylthiosemicarbazone-based ensemble of Hg2+ as selective fluorescence turn-on sensor toward cysteine in water. Tetrahedron Letters, 54(23), 2946-2951.

Mei J, Wang Y, Tong J, Wang J, Qin A, Sun JZ, Tang BZ, 2013. Discriminatory Detection of Cysteine and Homocysteine Based on Dialdehyde-Functionalized Aggregation-Induced Emission Fluorophores. Chemistry – A European Journal, 19(2), 613-620.

Niu L-Y, Guan Y-S, Chen Y-Z, Wu L-Z, Tung C-H, Yang Q-Z, 2012. BODIPY-Based Ratiometric Fluorescent Sensor for Highly Selective Detection of Glutathione over Cysteine and Homocysteine. Journal of the American Chemical Society, 134(46), 18928-18931.

Peng L, Zhou Z, Wei R, Li K, Song P, Tong A, 2014. A fluorescent probe for thiols based on aggregation-induced emission and its application in live-cell imaging. Dyes and Pigments, 108, 24-31.

Sok N, Nikolantonaki M, Guyot S, Nguyen TD, Viaux A-S, Bagala F, Rousselin Y, Husson F, Gougeon R, Saurel R, 2017. Design of new sensitive α,β-unsaturated carbonyl 1,8-naphtalimide fluorescent probes for thiol bioimaging. Sensors and Actuators B: Chemical, 242: 865-871.

Song H, Zhang J, Wang X, Zhou Y, Xu C, Pang X, Peng X, 2018. A novel "turn-on" fluorescent probe with a large stokes shift for homocysteine and cysteine: Performance in living cells and zebrafish. Sensors and Actuators B: Chemical, 259, 233-240.

Tong H, Zhao J, Li X, Zhang Y, Ma S, Lou K, Wang W, 2017. Orchestration of dual cyclization processes and dual quenching mechanisms for enhanced selectivity and drastic fluorescence turn-on detection of cysteine. Chemical Communications, 53(25), 3583-3586.

Wang F, Zhou L, Zhao C, Wang R, Fei Q, Luo S, Guo Z, Tian H, Zhu W-H, 2015. A dual-response BODIPY-based fluorescent probe for the discrimination of glutathione from cystein and homocystein. Chemical Science, 6(4), 2584-2589.

Wang J, Zhang F, Yang L, Wang B, Song X, 2021. A red-emitting fluorescent probe for sensing and imaging biothiols in living cells. Journal of Luminescence, 234, 117994.

Wang L, Zhuo S, Tang H, Cao D, 2018. An efficient fluorescent probe for rapid sensing of different concentration ranges of cysteine with two-stage ratiometric signals. Dyes and Pigments, 157, 284-289.

Wang Y, Zhu M, Jiang E, Hua R, Na R, Li QX, 2017. A Simple and Rapid Turn On ESIPT Fluorescent Probe for Colorimetric and Ratiometric Detection of Biothiols in Living Cells. Scientific Reports, 7(1), 4377.

Yue Y, Guo Y, Xu J, Shao S, 2011. A Bodipy-based derivative for selective fluorescence sensing of homocysteine and cysteine. New Journal of Chemistry, 35(1), 61-64.

Zhai D, Lee S-C, Yun S-W, Chang Y-T, 2013. A ratiometric fluorescent dye for the detection of glutathione in live cells and liver cancer tissue. Chemical Communications, 49(65), 7207-7209.

Zhang H, Liu R, Liu J, Li L, Wang P, Yao SQ, Xu Z, Sun H, 2016. A minimalist fluorescent probe for differentiating Cys, Hcy and GSH in live cells. Chemical Science, 7(1), 256-260.

Zhang J, Wang N, Ji X, Tao Y, Wang J, Zhao W, 2020. BODIPY-Based Fluorescent Probes for Biothiols. Chemistry – A European Journal, 26(19), 4172-4192.